Published in final edited form as:
Biotechnol Prog. 2010 ; 26(5): 1382–1390. doi:10.1002/btpr.435.

Scaffold Stiffness Affects the Contractile Function of Three-Dimensional Engineered Cardiac Constructs

Anna Marsano,
Dept. of Biomedical Engineering, Columbia University, New York, NY 10032

Robert Maidhof,
Dept. of Biomedical Engineering, Columbia University, New York, NY 10032

Leo Q. Wan,
Dept. of Biomedical Engineering, Columbia University, New York, NY 10032

Yadong Wang,
Dept. of Bioengineering, University of Pittsburgh, Pittsburgh, PA 15219

Jin Gao,
Dept. of Bioengineering, University of Pittsburgh, Pittsburgh, PA 15219

Nina Tandon, and
Dept. of Biomedical Engineering, Columbia University, New York, NY 10032

Gordana Vunjak-Novakovic
Dept. of Biomedical Engineering, Columbia University, New York, NY 10032

Abstract

We investigated the effects of the initial stiffness of a three-dimensional elastomer scaffold—highly porous poly(glycerol sebacate)—on functional assembly of cardiomyocytes cultured with perfusion for 8 days. The polymer elasticity varied with the extent of polymer cross-links, resulting in three different stiffness groups, with compressive modulus of 2.35 ± 0.03 (low), 5.28 ± 0.36 (medium), and 5.99 ± 0.40 (high) kPa. Laminin coating improved the efficiency of cell seeding (from 59 ± 15 to 90 ± 21%), resulting in markedly increased final cell density, construct contractility, and matrix deposition, likely because of enhanced cell interaction and spreading on scaffold surfaces. Compact tissue was formed in the low and medium stiffness groups, but not in the high stiffness group. In particular, the low stiffness group exhibited the greatest contraction amplitude in response to electric field pacing, and had the highest compressive modulus at the end of culture. A mathematical model was developed to establish a correlation between the contractile amplitude and the cell distribution within the scaffold. Taken together, our findings suggest that the contractile function of engineered cardiac constructs positively correlates with low compressive stiffness of the scaffold.

Keywords

scaffold; perfusion bioreactor; cardiac tissue engineering; mathematical model

Correspondence concerning this article should be addressed to G. Vunjak-Novakovic at gv2131@columbia.edu.
Anna Marsano and Robert Maidhof contributed equally to this work.

Additional supporting information may be found in the online version of this article.

Introduction

Cardiac tissue engineering can provide functional three-dimensional constructs to be used either for restoring heart function or as an in vitro model for studying cardiac development and disease. A common approach is to combine cells—primary cardiomyocytes[1,2] or their precursors derived from adult or embryonic stem cells[3,4]—with biomaterials and to apply biochemical and biophysical cues—such as mechanical stretch[5] or electrical stimulation[6,7]—to regulate tissue development.

An important consideration in this process is the selection of a biomaterial scaffold that serves as a three-dimensional template for directing cell attachment, differentiation,[8,9] organization,[10] and functionality.[11] An ideal biomaterial for cardiac tissue engineering should be biocompatible, safely degradable, have pores large enough to support the cells and allow cell interconnectivity, and have mechanical properties that resemble the native cardiac tissue.[12] Poly(Glycerol Sebacate) (PGS) meets many of these demands, and has been used for both vascular[13] and cardiac tissue engineering.[11,14] PGS is a tough elastomer with controllable mechanical properties that can be processed into scaffolds with high porosity (>90%), and large (150–200 μm) interconnected pores. As shown in our previous studies,[15,16] PGS can also be processed into scaffolds with arrays of channels for medium flow, thereby enabling efficient control of oxygen supply while protecting the cells from nonphysiologic hydrodynamic shear stress.

In vitro, the stiffness of the initial scaffold is expected to influence the progression of cell differentiation and assembly into engineered cardiac tissue. It has been shown that the differentiation status of a skeletal myoblast can be directly influenced by the stiffness of the substrate it is grown on, and that the myotubes cultured in two-dimensional (2D) settings differentiated optimally on materials with a stiffness mimicking that of native tissue.[8] It was postulated that a myocardium-like elasticity enables actomyosin striation and effective transmission of contractile work between the cells and the matrix.[17] In vivo, the mechanics of cell microenvironment also plays a key role in directing cell fate. The stiffness of infarcted myocardial tissue changes with time from soft to rigid, as the collagenous scar forms, a factor that is likely to determine the success of stem cell transplantation or cardiac patch implantation into the infarcted heart.[18] Presumably, there is a specific state of myocardial remodeling in which the biochemical and mechanical environment within the infarct bed is most suitable for supporting the recovery of the contractile function of the ventricle by transplanted cells.

We hypothesized that the in vitro development of engineered cardiac tissue from isolated cells on a three-dimensional (3D) scaffold will depend on the initial scaffold stiffness. We tested this hypothesis by culturing neonatal rat cardiomyocytes on PGS scaffolds with a range of compressive stiffnesses, with the application of laminin coating (to enhance cell attachment) and medium perfusion (to enhance oxygen supply to the cells necessary for their viability and function in thick tissue constructs).

Materials and Methods

PGS prepolymer synthesis

The synthesis of PGS was performed according to a previously published method.[13] Briefly, equimolar amounts of glycerol and purified sebacic acid were mixed in a 500-mL three-neck flask equipped with a N_2 bubbler, a thermocouple adaptor, and a Dean–Stark trap. The reaction was kept at 120°C under N_2 for 22 h. The N_2 bubbler was then removed, a vacuum line was attached, and the reaction mixture was kept at 100 mTorr and 120°C for another 52

h. The resulting PGS prepolymer was a pale yellow, highly viscous liquid (M_n = 9.6 kDa, PDI = 9.3).

PGS scaffold preparation

PGS scaffolds of three different stiffnesses have been generated as in our previous studies[16] by varying the polymer curing time. The curing times of 12, 32, and 36 h at 150°C resulted in PGS scaffolds with a low, medium, and high compressive stiffness.

PGS scaffold storage and sterilization

For storage time of up to 3 months, the PGS scaffolds were kept in a closed jar with a desiccant to maintain their dry state. Before use, the scaffolds were cored using an 8 mm biopsy punch, autoclaved (20 min at 121°C), and soaked in a series of 70, 50, and 25% ethanol solutions (15 min each), PBS (15 min), and in culture medium (overnight) to remove the unreacted monomers and condition the scaffold surface.

Laminin coating

For coated groups, scaffolds were incubated for 2 h at 37°C in a solution of 10 μg/mL laminin immediately following the PBS rinsing step, rinsed with sterile water to remove unattached laminin and soaked in culture medium overnight.[19]

Cell isolation

Cardiomyocytes were isolated from 2 day-old Sprague Dawley rats (Harlan) as previously described[16] according to an IACUC approved protocol. Briefly, ventricles were quartered, incubated at 4°C in a 0.06% (w/v) solution of trypsin in Hank's balanced salt solution (HBSS, Gibco), and subjected to a series of digestions (3–4 min, 37°C, 150 rpm) in a 0.1% (w/v) solution of collagenase type II in HBSS. Cell suspensions from the 4–5 digestions were collected and pre-plated in polystyrene culture flasks for a 75-min period to enrich for cardiomyocytes. The nonadherent cells were collected and counted using a hemocytometer.

Scaffold seeding with cells

Cardiomyocytes were seeded at a density of 1.35×10^8 cells/cm^3 into disk-shaped scaffolds (8 mm outer diameter × 1 mm thickness), by perfusing cell suspension through the inner 5 mm scaffold core for 2 h, as previously described.[16,20] Scaffolds were placed in custom-designed perfusion cartridges and held in place by silicone gaskets, directing the culture medium to flow through the inner 5 mm core of the scaffolds (Figure 1A). Medium perfusion (1 mm/s flow velocity, alternating flow direction every 2 min for 2 h) causes cells to become entrapped in the PGS pores. Immediately after seeding, a 2.5 mm biopsy punch was used to core out the central part of the scaffold, and obtain a ring-shaped construct (2.5 mm inner diameter, 5 mm outer diameter of the uniformly seeded region, and an 1.5 mm outer edge held by a gasket).

Construct culture

The ring-shaped constructs were cultured with medium perfusion[21] in high glucose DMEM supplemented with 10% fetal bovine serum for 8 days. During cultivation, the constructs were loosely confined between a polycarbonate ring and a removable placement cap that allowed the constructs to contract without floating away due to the flow. In this configuration, the seeded inner core (5 mm diameter) was exposed to medium that flowed through the inner 2.5 mm diameter hole (Figure 1B). A flow rate of 83 μm/sec through the central hole of the scaffold was used, with alternating flow direction after every 10 min for the duration of the 8-day culture period.

Assessments

DNA quantification

One half of each construct (n = 6 per group) was digested overnight at 56°C in 1 mL of 1 mg/mL proteinase K solution (pH 7.5), prepared in 10 mM Tris with 1 mM EDTA (from Sigma-Aldrich, St Louis, MO). All samples were then analyzed by using Quant-iT™ PicoGreen® dsDNA Assay Kit (Invitrogen Corporation, CA), according to the manufacturer's protocol.

Cell seeding efficiency

The seeding efficiency, defined as the percentage of initially seeded cells that attached to the scaffolds, was determined by comparing the DNA content present in each scaffold after 2 h of perfusion seeding to the reference DNA value determined for aliquots of the seeding cell suspension. For reference samples, cells were centrifuged to obtain pellets, digested with proteinase K solution, and analyzed using the PicoGreen assay. As these samples contained the same number of cells initially seeded per scaffold, they served as a reference (100% value) for seeding efficiency. For cultured cardiac constructs, samples were cut in half and weighed, digested with proteinase K solution, and analyzed using the PicoGreen assay. The linear relationship of the PicoGreen fluorescence with the cell number allowed us to directly calculate the seeding efficiency as the ratio of measured values.

Histology

For histological analysis, one half of each scaffold was fixed overnight in 4% neutral buffered formalin, embedded in paraffin, sectioned in 5 μm thick sections through the 1 mm thick cross-section of the scaffold, and stained with hematoxylin and eosin (H&E). Color images were acquired by Q-imaging camera mounted to a light microscope (Olympus).

Scaffold porosity

The porosity of each scaffold was determined using the following equation[13]:

$$\text{Porosity}(\%)=(\rho_{\text{PGS}}-\rho_{\text{d}})/\rho_{\text{PGS}} \times 100\%$$

For each scaffold, the dry mass and thickness were recorded after lyophilization, and the apparent scaffold density (ρ_{d}) was calculated from the scaffold dry weight and volume, where ρ_{PGS} was the density of nonporous PGS polymer which was 1.2 g cm^{-3} at 25°C. Results of three measurements for each scaffold (n = 5 scaffolds) were averaged.

Mechanical properties in compression

The mechanical properties were evaluated using a Synergie 100 mechanical analyzer equipped with a 50 N load cell as previously described.[13] Briefly, disc-shaped samples (9.52 mm in diameter × 1 mm thick) were cut, autoclaved 20 min, rinsed with 70, 50, 25 ethanol, and PBS, 15 min each, then evaluated while wet. Each sample was preloaded at 0.1 N, and compressed three times at 10% increments, up to the final strain of 30%, at a rate of 1.00 mm/min. The test results for each sample and compression cycle were averaged (n = 3), and the compression modulus was determined as the slope of the stress strain curve at 30% strain. The measured values were divided by (1 − ε), where ε is the scaffold porosity, to normalize for the differences in scaffold porosity.

Mechanical properties in axial tension

The tensile properties of PGS scaffolds were tested using an Instron Microtester 5848 (Instron, Norwood, MA, USA). The dry scaffold was cut into rectangular strips (40 mm long × 6 mm wide × 1 mm thick), autoclave-sterilized as described above, and evaluated while wet. The sample length and width were measured using a caliper, and the thickness was determined using an electronic digital micrometer (model 302M; Boecheler, Tuscon, AZ, USA). The wet samples were held by adjustable spring clamps at each end, a preload of ~0.02 N was applied and the samples were stretched at an axial speed of 0.2%, using two experimental protocols. In the first protocol, tension until rupture was measured, the force response was recorded, and the elastic modulus was calculated as the slope of the stress strain curve at 30% strain. The measured values were divided by $(1 - \varepsilon)$ to normalize for the differences in scaffold porosity. In the second protocol, tension until 20% strain was followed with the removal of force. The two stress–strain curves were compared to determine whether the matrices are elastomeric.

Contractile behavior of engineered constructs

Contractile activity of the engineered constructs in response to electrical field stimulation was assessed after 8 days of culture, by measuring the excitation threshold (the minimum stimulation voltage required for synchronous contraction) and the maximum capture rate (the maximum beating frequency that could be induced by electrical pacing), using methods established in our lab.[7] The amplitude of contraction (fractional area change) was also measured from videos of paced constructs by using a custom Matlab program.[7]

Implantation in an Animal Model of Cardiac Ischemia

We have developed a rat model of infarction secondary to total coronary occlusion for implantation of a cardiac patch. Briefly, the left anterior descending coronary artery (LAD) was exposed through a left thoracotomy. A prolene suture is passed around the LAD and tied. Following ischemia, PGS scaffolds (1 cm diameter × 1 mm thick discs, high and low stiffness groups) were sutured onto the infarct bed. The duration of implantation was 2 weeks, and the perioperative mortality was under 10%.

Mathematical modeling of contractile behavior

To understand the effects of the construct shape and cell distribution on the contractile behavior of engineered constructs, a simple mathematic model was developed and solved using COMSOL Multiphysics 3.3 (Burlington, MA, USA). Elastic response of the construct was analyzed by modeling the strain distribution at the state of maximum construct contraction.

As the thickness of the sample is relatively small compared with the sample diameter, the out-of-plane stresses (σ_z, σ_{rz}, and $\sigma_{\theta z}$) approximate zero, and the plane stress model could be adopted. Engineered constructs were assumed to be linearly elastic, with a Young's modulus (E) of 5 kPa, a value corresponding to the measured tensile modulus of the medium-stiffness scaffold group. For such porous scaffolds, the Poisson's ratio ν, defined as the ratio of transverse strain perpendicular to the applied load to the axial strain in the direction of applied load, ranges from 0 to 0.5, with 0 representing maximum compressibility (i.e., zero transverse strain under axial loading) and 0.5 representing incompressible material (i.e., no volumetric change under mechanical loading). An intermediate value $\nu = 0.25$ was chosen for mathematical modeling. With these assumptions, the constitutive relations between in-plane strains (ε_r, ε_θ, and $\varepsilon_{r\theta}$) and stresses (σ_r, σ_θ, and $\sigma_{r\theta}$) could be written as:

$$\varepsilon_r - \varepsilon_0 = (\sigma_r - \nu\sigma_\theta)/E \quad (1)$$

$$\varepsilon_\theta - \varepsilon_0 = (-\nu\sigma_r + \sigma_\theta)/E \quad (2)$$

$$\varepsilon_{r\theta} = 2\sigma_{r\theta}(1+\nu)/E \quad (3)$$

where ε_0 represented an initial isotropic stain (analog to thermal strain) because of the contractility of cardiomyocytes, which was assumed to be proportional to local cell density. For the axially symmetric case analyzed here, the governing equations for the state of plane stress are:

$$\delta\sigma_r/\delta_r + (\sigma_r - \sigma_\theta) = 0 \quad (4)$$

$$\delta\sigma_{r\theta}/\delta_r + 2\sigma_{r\theta}/r = 0 \quad (5)$$

Free boundaries were assumed at the inner ($r = r_{in}$) and outer ($r = r_{out}$) ring edges with:

$$\sigma_r = 0 \quad \text{and} \quad \sigma_{r\theta} = 0 \text{ at } r = r_{in} \quad (6)$$

$$\sigma_r = 0 \quad \text{and} \quad \sigma_{r\theta} = 0 \text{ at } r = r_{out} \quad (7)$$

As the actual cell distribution is dependent upon nutrient transport, we modeled cell density as a function of distance from the wall of the inner core.

To determine cell distribution, after 8 days of perfusion culture, H&E stained cross sections were imaged and divided into five equal 500 μm long segments, starting from the wall of the inner core. For each segment, the number of cells was counted and the local cell density was calculated. The average cell density over the entire section was also determined, and the corresponding cell contractility was assumed to be −0.1%. The local contractility (i.e., ε_0) profile was then obtained for each segment in proportion to the measured local cell density.

With Eqs. 1 and 2 and the obtained contractility profile, strain distributions (σ_r, σ_θ, and $\sigma_{r\theta}$) in the construct were calculated with COMSOL, using triangular meshes and the linear UMFPACK solver.

Statistical analysis

Parametric student's *t*-test (with normal population and equal variances) was used to determine statistical significance between samples. Results with $P < 0.05$ were considered significant.

Results

By varying the polymer curing time, we generated three groups of poly(glycerol-sebacate) (PGS) scaffolds with different mechanical properties in compression and tension (Figure 2A,B) and different porosity. The low, medium and high PGS stiffness groups had respectively a tensile modulus of 34.55 ± 1.26, 86.90 ± 3.59, and 167.76 ± 26.72 kPa and a compressive modulus of 2.35 ± 0.03, 5.28 ± 0.36, and 5.99 ± 0.40 kPa (in the low end of the range of elasticity of developing passive myocardium[17]).

To confirm that the scaffolds remain elastomeric after the curing process, mechanical properties were measured in tensile tests at large deformations (20% strain), with cycles of loading and unloading. In all cases, the scaffolds returned to their original shape after the force had been removed, and had comparable stress–strain profiles during the loading and unloading phase (Supporting Information Figure 1).

The porosity of the low, medium, and high stiffness groups was 76, 89, and 90%, respectively. Curing time had a significant impact on scaffold morphology and the physical and mechanical properties.[14] As the curing time increased, the scaffolds' dimensions were closer to those of the mold, and the moduli of the scaffolds increased. When curing time was 36 h, the scaffolds effectively maintained their dimensions without shrinking upon salt leaching and lyophilization. The scaffolds with a curing time of 12 h were significantly cohesive and adhesive, deformed much more easily due to insufficient crosslinking, and had smaller scaffold volumes, and therefore, higher polymer densities and lower porosities.

Low and high stiffness PGS scaffolds (acellular) were successfully implanted in the rodent model of cardiac infarction, without infection or adverse reaction to the elastomer implantation. Both the low and high stiffness scaffolds were easy to suture, without tears or breakdown of the material. At the time of the explant (2 week time point, Figure 3A–D), the scaffolds were partially degraded but still in place. A fibrous capsule formed around the site of the implantation, which is considered normal at 2 weeks after implantation. All the implants were well integrated with the surrounding tissue and contained infiltrating cells; therefore, PGS scaffolds in the studied stiffness range seem appropriate for future implantation studies.

Laminin-coating of PGS scaffolds before cell seeding markedly improved cell attachment, construct cellularity, and contractile behavior. On noncoated PGS scaffolds, the low, medium, and high stiffness scaffolds had seeding efficiencies of 59 ± 15, 68 ± 28, and 76 ± 9%, respectively. Laminin coating of low stiffness scaffolds resulted in an increase of cell seeding efficiency from 59 ± 15 to 90 ± 21% (Figure 4A). The increased seeding densities clearly correlated with the enhanced cell attachment and less-round cells on laminin-coated surfaces (Figure 4D,E). After 8 days of perfusion culture, SEM analysis showed that cells deposited more extracellular matrix in laminin-coated scaffolds (Figure 4F,G). The total DNA content was also significantly higher in laminin-coated constructs (Figure 4B). Most importantly, significant increase in contractility was observed for constructs grown using laminin-coated scaffolds, as evidenced by increased amplitudes of contraction both on the inner and outer edges of the constructs (Figure 4C). Based on these results, all scaffolds in further experiments were coated with laminin before cell seeding.

Following 8 days of perfusion culture, the constructs in each of the three stiffness groups maintained their ring shape but became more compact, especially on the inner edge of the ring. From the histology sections, we observed that in the low and medium stiffness scaffolds cells were producing matrix through the entire 1 mm thick cross section, but were present in greater abundance towards the inner edge of the ring (Figure 5A,B). In the high stiffness scaffolds, cells were markedly sparser and produced markedly less extracellular matrix, as assessed histologically (Figure 5C).

Total DNA content, contraction amplitude, and compressive modulus were measured for constructs in each of the three groups after 8 days of perfusion culture (Figure 6). The total DNA per construct was significantly higher in the low and medium stiffness group than in the high stiffness group (Figure 6A), a result corroborating histological findings (Figure 5). Consistently, the amplitude of contraction decreased with an increase in scaffold stiffness (Figure 6B). In all groups, the contraction amplitude was higher at the inner edge of the ring

(where cell density was greatest) than at the outer edge (Figure 6B). The fold of increase in the stiffness of engineered constructs, after 8 days of culture, was also highest for the constructs grown using low stiffness scaffolds (Figure 6C).

Finally, we constructed a mathematical model of our engineered constructs based on the actual cell distribution observed in the cultured tissue (Figure 7). Although the amplitude of contraction was higher at the inner than at the outer edge, the entire volume of the construct contracted in response to electrical field pacing, and the contractions of the inner and outer edge were in phase with one another (Figure 7A). As measured, 30 ± 1.7% of the cells were located within the interior 500 μm wide region of the ring, and the percentage of cells in each region decreased with distance from the inner edge. Very few cells were located beyond the 2.5 mm wide region from the interior edge, and for the modeling purposes we assumed no cells to be located beyond this point (Figure 7B).

The model predicted that the majority of radial strain in the construct occurs in the region of highest cell density, and that the radial strain decreases with the distance from the inner edge, as the cell density decreased. This is consistent with the measurements of the fractional area change that decreased from the inner edge to the outer edge. As a control case, we modeled the contractile behavior of a construct with spatially uniform cell distribution and showed that in this case the radial strain does not vary with the distance from the inner edge to the outer edge. The combined results of measurements and mathematical modeling therefore suggest that the differences in fractional area change between the inner and outer edges are because of the nonuniform cell distribution and not the construct shape.

Discussion

Although it has been shown that substrate stiffness plays a critical role in the development of engineered tissues, it is still difficult to translate the previous work performed in two dimensional culture systems[8] into three dimensional engineered tissue constructs. For two-dimensional substrates, the stiffnesses of ~1 and ~17 kPa were, respectively, below and above the optimal range for muscle cell differentiation.[8] In three-dimensional constructs, scaffold stiffness was shown to direct the organization of differentiated myoblasts.[22] Our study investigated the effect of scaffold mechanical properties on the formation of engineered cardiac tissue, using neonatal rat cardiac myocytes cultured on PGS scaffolds of three different stiffnesses in a bioreactor with medium perfusion (Figure 1).

We chose to use ring-shaped scaffolds based on earlier results where ring-shaped constructs had greater beating amplitude and higher cell density and extracellular matrix deposition than disc-shaped constructs.[23] As in this previous study, an 8-day culture period was long enough to allow the assembly of contractile cardiac constructs. To limit the expose of cells to hydrodynamic shear, we chose a relatively low flow rate (83 μm/sec), previously shown to support the development of engineered cardiac constructs.[24]

Biocompatibility studies of PGS scaffolds, by implantation into rat heart ventricles, gave results consistent with previously demonstrated biocompatibility of PGS material.[25] Both the high and low stiffness scaffolds were readily sutured to the heart wall in a rat infarction model, without any apparent tearing or damage to the scaffolds. Two weeks after implantation the scaffolds had begun to integrate with the ventricle wall, with blood vessels extending into the scaffold pores in both groups (Figure 3), suggesting that PGS scaffolds in this stiffness range were appropriate for implantation. The cell-adhesion properties of PGS scaffolds can be enhanced by coating with adhesive proteins or by grafting hydrophobic moieties to the hydroxyl groups.[25] In a study with rat aortic endothelial cells, coating PGS

scaffolds with laminin (a protein found in the matrix of many tissue types, including cardiac muscle) resulted in significantly higher DNA content and proliferating cell percentage, lower apoptotic cell percentage, and a more spread cell morphology.[19] Laminin coating in conjunction with 5-azacytidine supplementation enhanced the commitment of stem cells toward a cardiac lineage.[26] Thus, we expected that laminin coating would enhance the functionality of engineered cardiac tissues through positive effects on cell spreading and integration with the scaffold material. As expected, an improvement over using no coating was seen in laminin-coated scaffolds in terms of cell seeding efficiency and matrix deposition and most notably the contractile properties of the engineered tissues (Figure 4). Throughout the culture, the cells reside in a 3D environment—initially within cell aggregates and subsequently by interacting with the scaffold and the newly synthesized matrix.

Scaffold stiffness proved to be a key determinant of the functional properties of engineered cardiac tissue. Stiffness and porosity differences between the groups did not affect the seeding efficiency. All three stiffness groups promoted tissue formation and the development of synchronous contractions, but the greatest amplitude of contraction was found with low stiffness PGS. In the high stiffness group, extracellular matrix was sparse and the final cell density was low (Figure 5), resulting in poor contractility compared to other groups (Figure 6).

Curing of the PGS prepolymer leads to reactions between the residual OH and COOH groups, and can thereby change surface properties. As stiffer scaffolds are likely to have less unreacted OH and COOH groups than soft scaffolds, curing can result in some differences in the surface properties of the scaffold groups, which in turn may affect laminin coating and the cell behavior. However, as only a molecular layer of laminin is deposited on the scaffold surface, there should be no effect of laminin on scaffold stiffness.

The cells constantly respond to the matrix stiffness, in vitro and in vivo, in a process that can be described as dynamic reciprocity.[12] Interestingly, the Young's modulus in compression was highest for constructs that started with the lowest stiffness PGS (Figure 6), reflective of the enhanced matrix deposition and cell spreading seen in this group. Consistent with previous studies,[8,17] there seem to be a window of the scaffold stiffness, which is optimal for the stimulation of contractile phenotype and functional cell assembly.

Adjustment of scaffold stiffness by curing time resulted in the concurrent change of scaffold porosity. The range of porosity of the three scaffold groups (76–90%) is suitable for tissue engineering applications, but there was a trend of change between the groups, with the stiffest scaffolds having the highest porosity. Because the higher porosity did not lead to higher cell density (Figures 4 and 6), it is reasonable to attribute the different construct outcomes to scaffold stiffness rather than porosity. Still, the two effects could not be completely separated in the present study. Moreover, longer curing time results in higher density of cross-links that also results in slower degradation of scaffold material by plain hydrolysis. On the other hand, PGS degradation is catalyzed by enzymes, a cell type dependent mechanism independent of the degree of crosslinking or stiffness of the scaffold.[27] Taken together, these findings suggest that differences in scaffold degradation were not significant for the results of the present study, because of the relatively short duration of both the in vitro and in vivo experiments, but may indeed be important for longer times of implantation.

In all stiffness groups the area change measured at the inner edge of the constructs was greater than that measured at the outer edge. There were two possible reasons for this effect: (1) nonuniform cell distribution favoring a higher cell density at the inner edge, and (2) the

ring-shaped geometry allowing for greater contraction amplitude at the inner core. Greater cell density was observed towards the central part of the ring-shaped constructs, likely an effect of flow and increased nutrient transport near the central hole. By mathematical modeling we compared the effects on contractile amplitude of the actual cell distribution to a hypothetical spatially uniform distribution (Figure 7). For the uniform cell concentration case, shortening was the same at the inner and outer edges of the construct, whereas for the experimentally measured distribution shortening was greater at the inner edge of the ring, as we observed for our engineered constructs. Cell distribution thus plays a role in the development of contractile properties of engineered cardiac tissue, presumably because of the related effects to cell coupling.

Summary

In this study, we show that the stiffness and surface coating of elastomer scaffolds play major roles in the development of engineered cardiac tissue. Of the three groups tested, the lowest stiffness group (2.35 ± 0.03 kPa modulus in compression and 34.55 ± 1.26 kPa modulus in tension) resulted in engineered tissues with the greatest contraction amplitude, matrix deposition, and compressive modulus after 8 days of cultivation with medium perfusion. Greater contraction amplitude was observed at the inner edge than at the outer edge of the ring-shaped constructs, and a mathematical model created to analyze the contractile behavior demonstrated that the effect was because of the differences in cell density. In sum, soft elastomer scaffolds coated with laminin and cultured under conditions supporting high densities of viable cells enhanced the material properties and contractile behavior of engineered cardiac constructs.

Acknowledgments

The authors gratefully acknowledge the NIH funding of this work (HL076485, EB002520, and HL089913 to GVN; stipend from T 32 HL087745 to RM), and the help of Tim Martens and George Eng with harvesting rat hearts, Sarindr Bhumiratana with mechanical testing, and Darja Marolt with scientific discussions.

Literature Cited

1. Akins RE, Boyce RA, Madonna ML, Schroedl NA, Gonda SR, McLaughlin TA, Hartzell CR. Cardiac organogenesis in vitro: reestablishment of three-dimensional tissue architecture by dissociated neonatal rat ventricular cells. Tissue Eng. 1999; 5:103–118. [PubMed: 10358218]
2. Fink C, Ergun S, Kralisch D, Remmers U, Weil J, Eschenhagen T. Chronic stretch of engineered heart tissue induces hypertrophy and functional improvement. FASEB J. 2000; 14:669–679. [PubMed: 10744624]
3. Bursac N. Cardiac tissue engineering using stem cells. IEEE Eng Med Biol Mag. 2009; 28:80, 82, 84–86, 88–89. [PubMed: 19353830]
4. Ugurlucan M, Yerebakan C, Furlani D, Ma N, Steinhoff G. Cell sources for cardiovascular tissue regeneration and engineering. Thorac Cardiovasc Surg. 2009; 57:63–73. [PubMed: 19241306]
5. Zimmermann WH, Melnychenko I, Wasmeier G, Didie M, Naito H, Nixdorff U, Hess A, Budinsky L, Brune K, Michaelis B, Dhein S, Schwoerer A, Ehmke H, Eschenhagen T. Engineered heart tissue grafts improve systolic and diastolic function in infarcted rat hearts. Nat Med. 2006; 12:452–458. [PubMed: 16582915]
6. Genovese JA, Spadaccio C, Langer J, Habe J, Jackson J, Patel AN. Electrostimulation induces cardiomyocyte predifferentiation of fibroblasts. Biochem Biophys Res Commun. 2008; 370:450–455. [PubMed: 18384743]
7. Tandon N, Cannizzaro C, Chao PH, Maidhof R, Marsano A, Au HT, Radisic M, Vunjak-Novakovic G. Electrical stimulation systems for cardiac tissue engineering. Nat Protoc. 2009; 4:155–173. [PubMed: 19180087]

8. Engler AJ, Griffin MA, Sen S, Bonnemann CG, Sweeney HL, Discher DE. Myotubes differentiate optimally on substrates with tissue-like stiffness: pathological implications for soft or stiff microenvironments. J Cell Biol. 2004; 166:877–887. [PubMed: 15364962]
9. Evans ND, Minelli C, Gentleman E, LaPointe V, Patankar SN, Kallivretaki M, Chen X, Roberts CJ, Stevens MM. Substrate stiffness affects early differentiation events in embryonic stem cells. Eur Cell Mater. 2009; 18:1–13. discussion 13–14. [PubMed: 19768669]
10. Ishii O, Shin M, Sueda T, Vacanti JP. In vitro tissue engineering of a cardiac graft using a degradable scaffold with an extracellular matrix-like topography. J Thorac Cardiovasc Surg. 2005; 130:1358–1363. [PubMed: 16256789]
11. Radisic M, Park H, Martens TP, Salazar-Lazaro JE, Geng W, Wang Y, Langer R, Freed LE, Vunjak-Novakovic G. Pre-treatment of synthetic elastomeric scaffolds by cardiac fibroblasts improves engineered heart tissue. J Biomed Mater Res A. 2008; 86:713–724. [PubMed: 18041719]
12. Vunjak-Novakovic G, Tandon N, Godier A, Maidhof R, Marsano A, Martens T, Radisic M. Challenges in cardiac tissue engineering. Tissue Eng Part B Rev. 2010; 16:169–187. [PubMed: 19698068]
13. Gao J, Crapo PM, Wang Y. Macroporous elastomeric scaffolds with extensive micropores for soft tissue engineering. Tissue Eng. 2006; 12:917–925. [PubMed: 16674303]
14. Chen QZ, Bismarck A, Hansen U, Junaid S, Tran MQ, Harding SE, Ali NN, Boccaccini AR. Characterisation of a soft elastomer poly(glycerol sebacate) designed to match the mechanical properties of myocardial tissue. Biomaterials. 2008; 29:47–57. [PubMed: 17915309]
15. Radisic M, Deen W, Langer R, Vunjak-Novakovic G. Mathematical model of oxygen distribution in engineered cardiac tissue with parallel channel array perfused with culture medium containing oxygen carriers. Am J Physiol Heart Circ Physiol. 2005; 288:H1278–H1289. [PubMed: 15539422]
16. Radisic M, Marsano A, Maidhof R, Wang Y, Vunjak-Novakovic G. Cardiac tissue engineering using perfusion bioreactor systems. Nat Protoc. 2008; 3:719–738. [PubMed: 18388955]
17. Engler AJ, Carag-Krieger C, Johnson CP, Raab M, Tang HY, Speicher DW, Sanger JW, Sanger JM, Discher DE. Embryonic cardiomyocytes beat best on a matrix with heart-like elasticity: scar-like rigidity inhibits beating. J Cell Sci. 2008; 121:3794–3802. [PubMed: 18957515]
18. Zhang S, Sun A, Liang Y, Chen Q, Zhang C, Wang K, Zou Y, Ge J. A role of myocardial stiffness in cell-based cardiac repair: a hypothesis. J Cell Mol Med. 2009; 13:660–663. [PubMed: 19243474]
19. Lee EJ, Vunjak-Novakovic G, Wang Y, Niklason L. A biocompatible endothelial cell delivery system for in vitro tissue engineering. Cell Transplant. In press.
20. Wendt D, Marsano A, Jakob M, Heberer M, Martin I. Oscillating perfusion of cell suspensions through three-dimensional scaffolds enhances cell seeding efficiency and uniformity. Biotechnol Bioeng. 2003; 84:205–214. [PubMed: 12966577]
21. Grayson WL, Bhumiratana S, Cannizzaro C, Chao PH, Lennon DP, Caplan AI, Vunjak-Novakovic G. Effects of initial seeding density and fluid perfusion rate on formation of tissue-engineered bone. Tissue Eng Part A. 2008; 14:1809–1820. [PubMed: 18620487]
22. Levy-Mishali M, Zoldan J, Levenberg S. Effect of scaffold stiffness on myoblast differentiation. Tissue Eng Part A. 2009; 15:935–944. [PubMed: 18821844]
23. Marsano A, Maidhof R, Tandon N, Gao J, Wang Y, Vunjak-Novakovic G. Engineering of functional contractile cardiac tissues cultured in a perfusion system. Conf Proc IEEE Eng Med Biol Soc. 2008; 2008:3590–3593. [PubMed: 19163485]
24. Carrier RL, Rupnick M, Langer R, Schoen FJ, Freed LE, Vunjak-Novakovic G. Perfusion improves tissue architecture of engineered cardiac muscle. Tissue Eng. 2002; 8:175–188. [PubMed: 12031108]
25. Wang Y, Ameer GA, Sheppard BJ, Langer R. A tough biodegradable elastomer. Nat Biotechnol. 2002; 20:602–606. [PubMed: 12042865]
26. van Dijk A, Niessen HW, Zandieh Doulabi B, Visser FC, van Milligen FJ. Differentiation of human adipose-derived stem cells towards cardiomyocytes is facilitated by laminin. Cell Tissue Res. 2008; 334:457–467. [PubMed: 18989703]

27. Pomerantseva I, Krebs N, Hart A, Neville CM, Huang AY, Sundback CA. Degradation behavior of poly(glycerol sebacate). J Biomed Mater Res A. 2009; 91:1038–1047. [PubMed: 19107788]

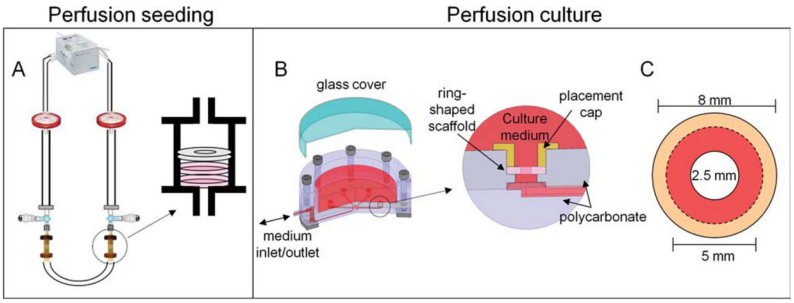

Figure 1. Overview of perfusion systems for ring-shaped cardiac constructs

Two disc-shaped PGS scaffolds were placed in perfusion cartridges, held in place with a silicone gasket, and connected via tubing in a loop configuration (A). A cardiac cell suspension was then perfused through the scaffold pores, leaving 8 mm diameter constructs with the inner 5 mm homogeneously seeded. Then the inner 2.5 mm of each scaffold was removed via biopsy punch. One ring-shaped construct was placed into each of the six bioreactor wells and held in place between a polycarbonate ring of the bioreactor and a removable placement cap (B). The central core of each scaffold (8 mm outer diameter, 2.5 mm inner diameter) was perfused, whereas the outer edge (dotted line) was held by the placement cap (C).

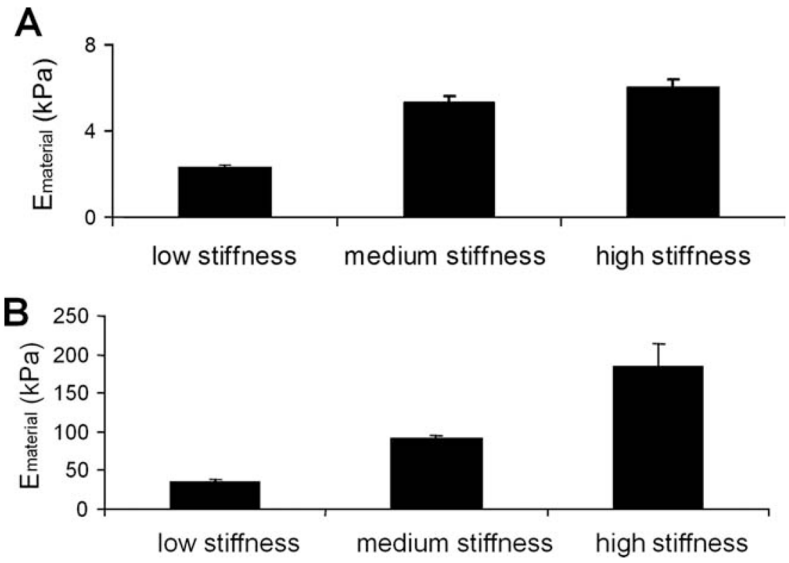

Figure 2. PGS mechanical properties

Graphs represent the PGS material modulus (E_m) in compression (A) and in tension (B).

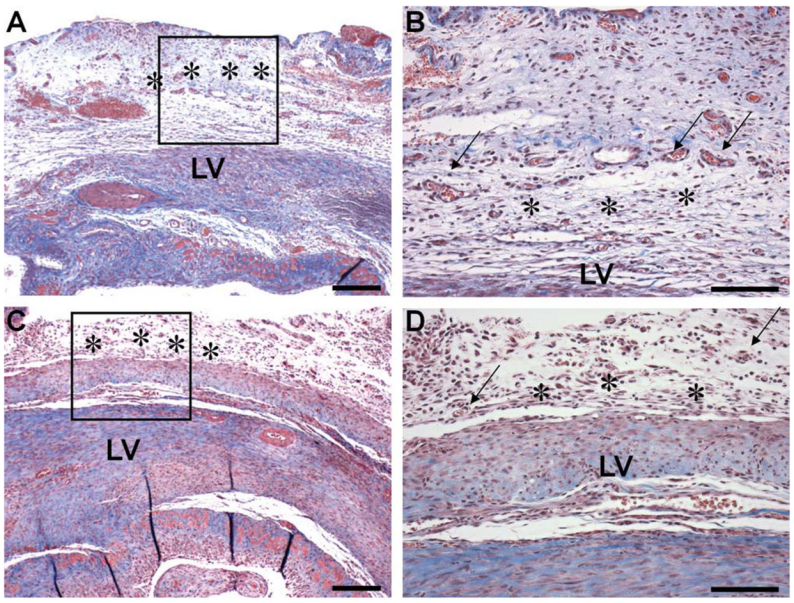

Figure 3. In vivo biocompatibility

Implantation of low (A, B) or high (C, D) stiffness PGS scaffolds in a rat after induction of myocardial infarction by permanent ligation of the anterior descending coronary artery. Histological images show the integration between graft (stars) and the left ventricle (LV) at 2 weeks. Note the formation of blood vessels (arrow) in the higher magnifications view (B, D). Stain: Trichrome. Scale bars: 0.25 mm (A, C) and 0.1 mm (B, D).

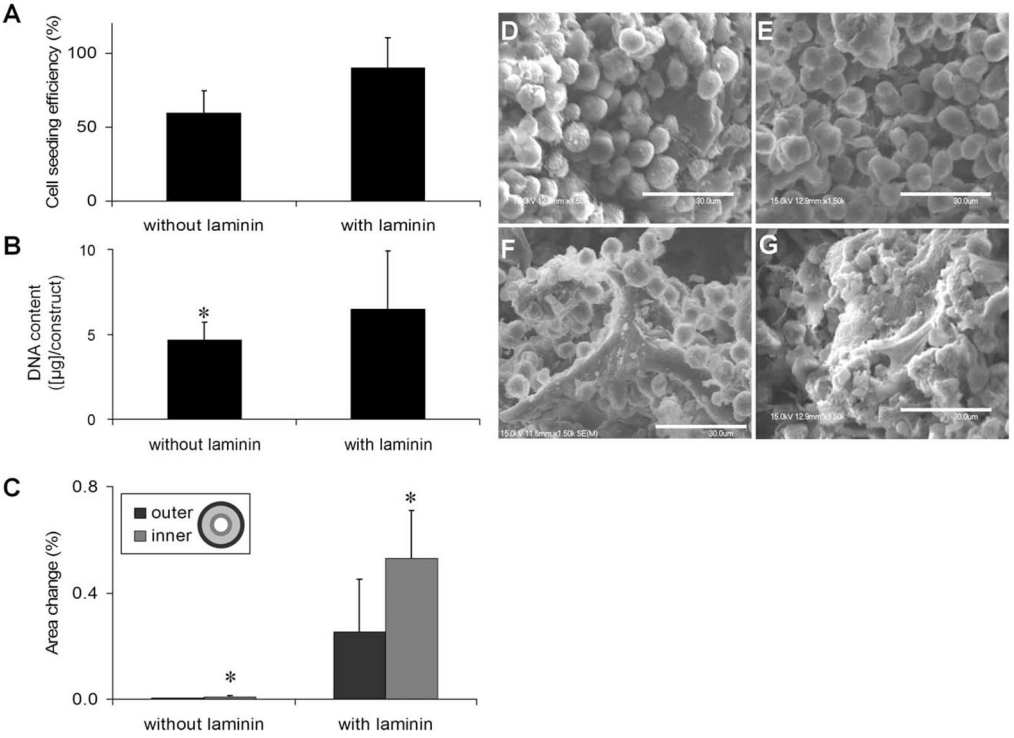

Figure 4. Cell seeding efficiency was assessed for cardiac constructs generated with low stiffness PGS scaffolds with (+L) or without (−L) laminin coating following 2-h perfusion seeding (A).< br>After 8 days of culture in perfusion, DNA content per construct ($P < 0.01$) (B) and the percentage of area change during pacing (* = means statistically different from all the other groups, $P < 0.05$) (C) were assessed for cardiac constructs generated starting with low stiffness scaffold previously coated with (+L) or without (−L) laminin. SEM images were acquired for constructs generated with low stiffness scaffolds with (E, G) or without (D, F) laminin coating following either 2-h perfusion seeding (D, E) or 8-day culture (F, G).

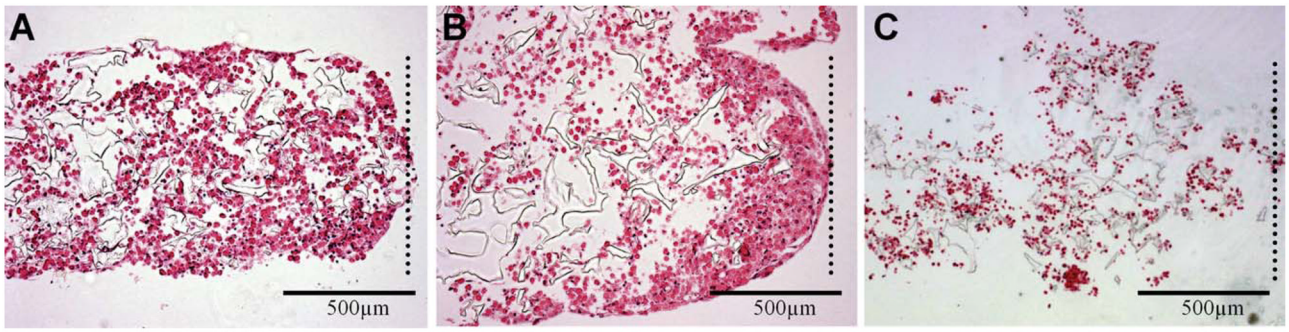

Figure 5. Hematoxylin and eosin stained histological sections of cardiac constructs generated with low (A), medium (B), and high (C) stiffness PGS scaffolds

Dotted lines indicate inner edge of the ring-shaped constructs.

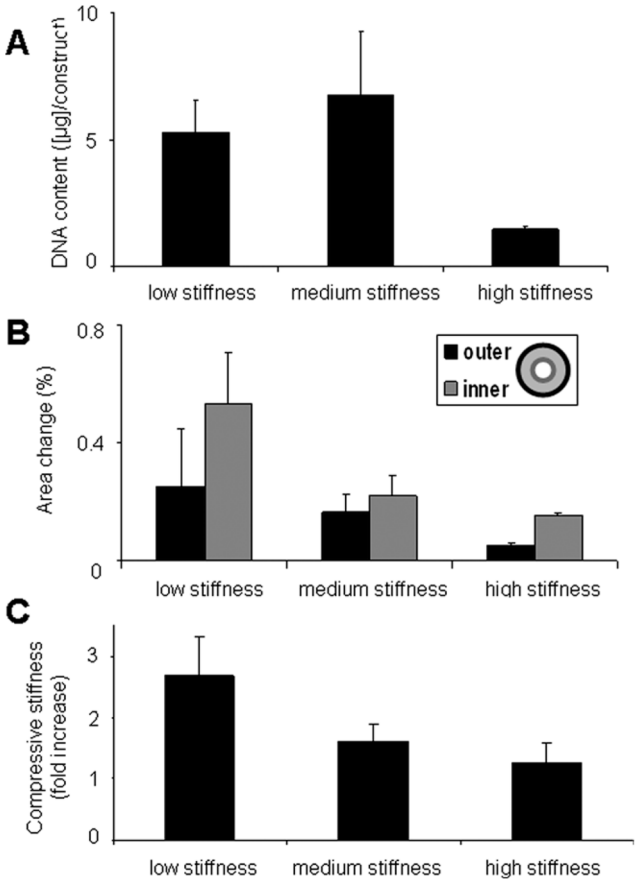

Figure 6. Following 8 days perfusion culture of laminin coated constructs the DNA content per construct was measured by PicoGreen assay (* = statistically different from all other groups, $P < 0.05$) (A)

The functionality of the different stiffness groups was assessed by measuring fractional area change of the inner and outer edges of the ring, as defined in the legend (* = statistically different from the results within the same other group, either outer or inner, $P < 0.05$) (B) and the modulus in compression was measured at 30% strain (C).

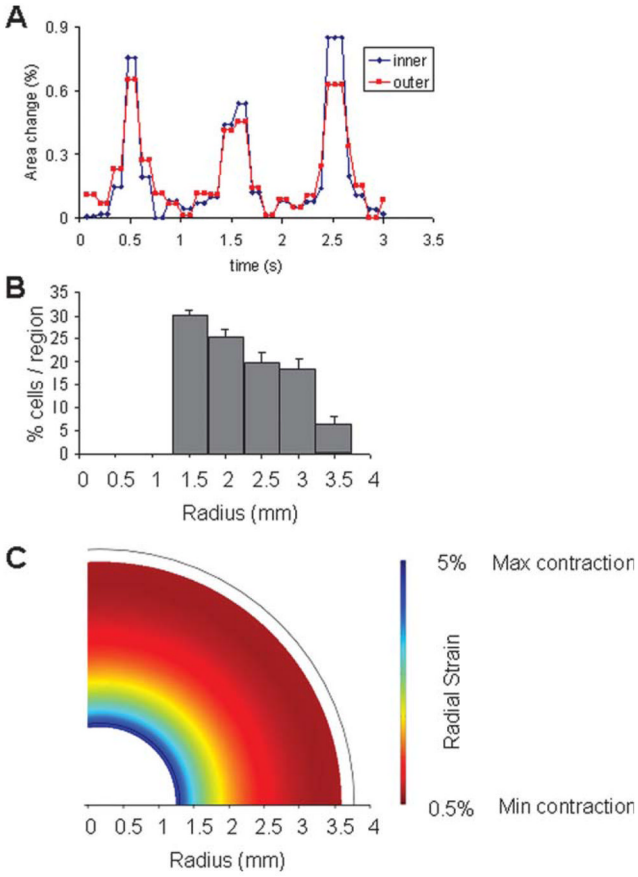

Figure 7. Representative area change measurement data showing synchronicity of contractions between the inner and outer edges of the ring-shaped scaffolds (Graph A)

Mathematical modeling of contractions for constructs with measured or uniform cell distributions. The experimental distribution (B) was measured as described and fit with a polynomial curve. Our model was then used to predict regions of shortening in the case of the observed cell distribution (C).